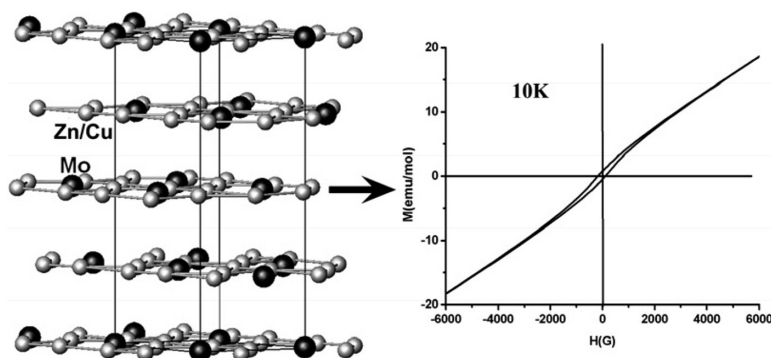


LaCuZnMoO: Zinc-Doped Cuprates with Kagomé Lattices

Li, You, Wei, Yue Lu, Jing Ju, Anders Wannberg, Hkan Rundlf, Zou, Tao Yang, Tian, Liao, Naoki Toyota, and Lin

J. Am. Chem. Soc., **2005**, 127 (40), 14094-14099 • DOI: 10.1021/ja053489a • Publication Date (Web): 17 September 2005

Downloaded from <http://pubs.acs.org> on March 25, 2009



More About This Article

Additional resources and features associated with this article are available within the HTML version:

- Supporting Information
- Access to high resolution figures
- Links to articles and content related to this article
- Copyright permission to reproduce figures and/or text from this article

[View the Full Text HTML](#)

La₄Cu_{3-x}Zn_xMoO₁₂: Zinc-Doped Cuprates with Kagomé Lattices

Guobao Li,* Liping You,[†] Wutao Wei,[‡] Yue Lu,[‡] Jing Ju,[§] Anders Wannberg,[#]
Håkan Rundlöf,[#] Xiaodong Zou,[¶] Tao Yang, Shujian Tian, Fuhui Liao,
Naoki Toyota,[§] and Jianhua Lin

Contribution from the State Key Laboratory of Rare Earth Materials Chemistry and Applications, College of Chemistry and Molecular Engineering, Peking University, Beijing 100871, P.R. China

Received May 28, 2005; E-mail: liguobao@pku.edu.cn

Abstract: Two solid solutions, La₄Cu_{3-x}Zn_xMoO₁₂ (0.05 ≤ x ≤ 0.20, SS1) and La₄Cu_{3-x}Zn_xMoO₁₂ (0.30 ≤ x ≤ 2.40, SS2), were synthesized at ambient pressure and at temperatures from 1025 to 1200 °C by traditional solid-state reactions. Their structures were determined from X-ray powder diffraction with the help of electron and neutron diffraction. The atomic arrangements of SS1 and SS2 are similar, but their space groups are different, *Pmnm* for SS1 and *P-1* for SS2, respectively. The copper, zinc, and molybdenum are coordinated by oxygen in corner-sharing trigonal bipyramids that are sandwiched between layers of lanthanum cations. In the transition metal cations layer of SS2, the copper and zinc cations order into a Kagomé-like lattice of triangular clusters. The magnetism has been measured from 2 to 300 K and is highly influenced by the geometric arrangement of the Cu^{II} and Zn^{II} cations. The number of free electrons per three Cu atoms is close to one for all samples in SS1 and SS2 indicating that the system can be well expressed by independent Cu^{II}₃ clusters. Spontaneous magnetization was observed in the system.

Introduction

Frustration is a phenomenon often seen in solid-state materials when conflicting requirements are present for establishing long-range order. Frustration of site disorder is a typical example of the structural disorder that becomes, for example, a key concept to describe spin glasses.¹ In addition, the geometrical constraint in some systems may also lead to frustration of interactions between the transition metal ions.²⁻⁹ The Kagomé lattice is a well-known example, in which the magnetic interactions of triangular clusters are frustrated, which has been the subject of many theoretical studies.¹⁰ A few real materials that can be

modeled as a Kagomé lattice include SrCr₈Ga₄O₁₉, Ba₂Sn₂Ga₃ZnCr₇O₂₂, and jarosites [KM₃(SO₄)₃(OH)₆, M = Fe^{III}, Cr^{III}, V^{III}].¹¹⁻¹³ Recently, an interesting geometrically frustrated system, La₄Cu₃MoO₁₂ (*P112₁/m*), was reported.¹⁴ The structure of this compound is closely related to that of the hexagonal YAlO₃, in which copper and molybdenum occupy trigonal bipyramid sites forming transition metal and oxygen sheets and lanthanum cations are located between the sheets.¹⁵ In a fully ordered structure, the copper cations comprise triangular clusters to form a 2D square lattice in the basal plane, in which the magnetic interactions between the copper ions are frustrated, leading to an antiferromagnetic transition at around 5 K.¹⁶ One might expect that the lanthanum, copper, and molybdenum in La₄Cu₃MoO₁₂ could be replaced by other lanthanides and transition metals, for example, Cu by Zn, Ni, Co, or Fe and Mo by W. Indeed isostructural compounds were reported for most of the lanthanides, Ln = Pr, Nd, Sm, Eu, Gd, Tb, Dy, Ho, Er, Dy, Yb, and Lu for Ln₄Cu₃MoO₁₂.¹⁷ However, there were no reports that show transition metal substitution of the Cu site in La₄Cu₃MoO₁₂. A known compound is La₄Ni₃MoO₁₂,

[†] Electron Microscope Lab, Peking University, Beijing 100871, P.R. China.

[‡] Students from The First High School attended to Beijing Normal University, Beijing, P.R. China.

[§] Physics Department, Graduate School of Science, Tohoku University, Sendai 980-8578, Japan.

[#] Studsvik Neutron Research Laboratory, Uppsala University, S-611 82 Nyköping, Sweden.

[¶] Structural Chemistry, Stockholm University, SE-10691 Stockholm, Sweden.

- (1) Binder, K.; Young, A. P. *Rev. Mod. Phys.* **1986**, *58*, 801.
- (2) Ramirez, A. P. *Handbook of Magnetic Materials*; Buschow, K. H. J., Ed.; Elsevier: Amsterdam, 2001; Vol. 13, p 423.
- (3) Canals, B.; Lacroix, C. *Phys. Rev. Lett.* **1998**, *80*, 2933.
- (4) Ramirez, A. P.; Hayashi, A.; Cava, R. J.; Siddharthan, R.; Shastry, B. S. *Nature (London)* **1999**, *399*, 333.
- (5) Bramwell, S. P.; Gringas, M. J. P. *Science* **2001**, *294*, 1495.
- (6) Garcia-Adeva, A. J.; Huber, D. L. *Phys. Rev. Lett.* **2000**, *85*, 4598.
- (7) Lee, S.-H.; Broholm, C.; Ratcliff, W.; Gasparovic, G.; Huang, Q.; Kim, T. H.; Cheong, S.-W. *Nature (London)* **2002**, *418*, 856.
- (8) Berg, E.; Altman, E.; Auerbach, A. *Phys. Rev. Lett.* **2003**, *90*, 147204.
- (9) Dagotto, E.; Rice, T. M. *Science* **1996**, *271*, 618-623.
- (10) Chalker, J. T.; Holdsworth, P. C. W.; Shender, E. F. *Phys. Rev. Lett.* **1992**, *68*, 855-858.

- (11) Obradors, X.; Labarta, A.; Isalgué, A.; Tejada, J.; Rodriguez, J.; Pernet, M. *Solid State Commun.* **1988**, *65*, 189.
- (12) Hagemann, I. S.; Huang, Q.; Gao, X. P. A.; Ramirez, A. P.; Cava, R. J. *Phys. Rev. Lett.* **2001**, *86*, 894.
- (13) Wills, A. S. *Phys. Rev. B* **2001**, *63*, 064430.
- (14) Vander Griend, D. A.; Vincent Caignaert, S. B.; Poeppelmeier, K. R.; Wang, Y. G.; Dravid, V. P.; Azuma, M.; Takano, M.; Hu, Zh. B.; Jorgensen, J. D. *J. Am. Chem. Soc.* **1999**, *121*, 4787-4792.
- (15) Bertaut, E. F.; Mareschal, J. *Compt. Rend.* **1963**, *257*, 867-70.
- (16) Wang, H. T. *Phys. Rev. B* **2001**, *65*, 024426.
- (17) Vander Griend, D. A.; Malo, S.; Wang, T. K.; Poeppelmeier, K. R. *J. Am. Chem. Soc.* **2000**, *122*, 7308-7311.

which, however, is a polymorph that crystallizes in a perovskite-related structure.¹⁸ Substitution study for the copper ions in $\text{La}_4\text{Cu}_3\text{MoO}_{12}$ is interesting since replacement of Cu^{II} ($S = 1/2$) by other transition metal cations M^{II} ($S \neq 1/2$) may tune the magnetic interaction. In this study, we report a study to substitute Cu by Zn. Two solid solutions, $\text{La}_4\text{Cu}_{3-x}\text{Zn}_x\text{MoO}_{12}$ ($0.05 \leq x \leq 0.20$, denoted as SS1) and $\text{La}_4\text{Cu}_{3-x}\text{Zn}_x\text{MoO}_{12}$ ($0.30 \leq x \leq 2.40$, denoted as SS2), were identified, and both of them crystallize in the YAIO_3 -related structures. SS2 crystallizes in a triclinic structure with a different ordered arrangement for Mo and Cu/Zn, where the Cu/Zn atoms form a Kagomé lattice. This structure is a new polymorph for this system, and the substitution of Cu by Zn leads to ferromagnetic ordering in this solid solution and decreases the conductivity (see the Supporting Information for details).

Experimental Section

Synthesis. Samples of $\text{La}_4\text{Cu}_{3-x}\text{Zn}_x\text{MoO}_{12}$ series ($x = 0.0, 0.05, 0.10, 0.15, 0.20, 0.25, 0.28, 0.30, 0.60, 0.80, 1.00, 1.30, 1.60, 2.00, 2.30, 2.60, 2.70, 2.80$) were synthesized at ambient pressure and high temperature. Stoichiometric amounts of starting materials, La_2O_3 (99.995%), CuO (AR), ZnO (AR), and MoO_3 (AR) were mixed and pressed into pellets (10 ton/cm^2) and then heated at a temperature in the range of $1025\text{--}1200 \text{ }^\circ\text{C}$ (see the Supporting Information for details) in air for 4 days with intermittent grindings. The temperatures should be carefully maintained, otherwise the lower x value samples ($\text{La}_4\text{Cu}_{3-x}\text{Zn}_x\text{MoO}_{12}$) may melt or even evaporate, whereas the high x value samples may not reach equilibrium. After cooling the samples at a rate of $30 \text{ }^\circ\text{C/h}$, dark gray to green-yellow samples of $\text{La}_4\text{Cu}_{3-x}\text{Zn}_x\text{MoO}_{12}$ were obtained. Most of the samples are single phases as confirmed by X-ray powder diffraction.

Characterizations. X-ray powder diffraction (XPD) data were recorded using a Rigaku D/Max-2000 diffractometer with graphite monochromatized Cu K α radiation at 40 kV, 100 mA. Powder diffraction data used for structure refinement were collected in the range of 5° to 120° with a step-scanning mode (step: 0.02). Neutron powder diffraction for the sample $\text{La}_4\text{Cu}_2\text{ZnMoO}_{12}$ was collected at room temperature, 50, and 10 K, respectively, at the Neutron Research Laboratory in Studsvik (NFL). The diffraction data at room temperature were collected on the R2D2 diffractometer (1.5514 \AA) in $5.80^\circ \leq 2\theta \leq 140^\circ$ with a step of 0.05° ; while the low-temperature data (50 and 10 K) were collected on the NPD diffractometer (1.470 \AA) in $4.00^\circ \leq 2\theta \leq 140^\circ$ with a step of 0.08° . For electron diffraction study, the samples were ground in an agate mortar and dispersed in acetone, and fragments of the crystallite were collected on a holey carbon film supported on a copper grid. Selected area electron diffraction (SAED) and high-resolution electron microscopy (HREM) were carried out on an H-9000 transmission electron microscope at 300 kV.

Structural Characterization. X-ray powder diffraction patterns of SS1 and SS2 solid solutions are quite similar to the monoclinic $\text{La}_4\text{Cu}_3\text{MoO}_{12}$ (m - $\text{La}_4\text{Cu}_3\text{MoO}_{12}$). Therefore, initially we refined the structures with a monoclinic model using GSAS.^{19,20} Although the fit of the X-ray diffraction patterns is quite good, there are several weak reflections that cannot be indexed with the monoclinic cell. Careful examination of electron diffraction revealed that SS1 crystallizes in the high-temperature orthorhombic structure of $\text{La}_4\text{Cu}_3\text{MoO}_{12}$, while the sym-

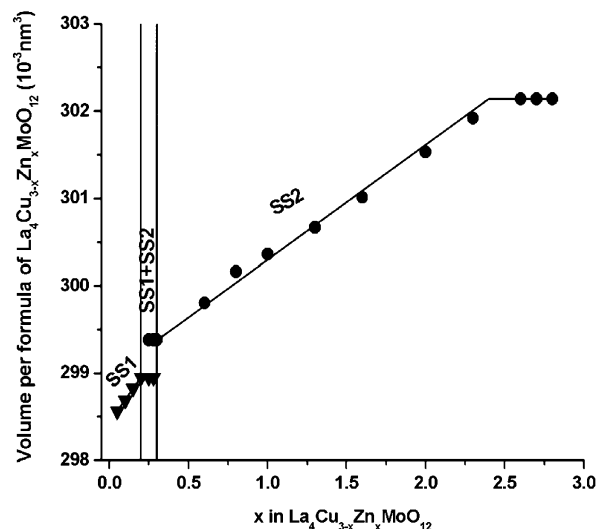


Figure 1. Unit cell volume as a function of the composition of $\text{La}_4\text{Cu}_{3-x}\text{Zn}_x\text{MoO}_{12}$; the solid solution SS1 is in the range of $0.05 \leq x \leq 0.20$, SS2 is in the range of $0.30 \leq x \leq 2.40$, and between consists of a two-phase region.

metry of SS2 is lower and can only be described in the triclinic structure. In fact, the three structures have the same structural framework but have different arrangements of Mo and Cu/Zn atoms.

Magnetic Measurements. Magnetic measurements were performed using a Quantum Design physical property measurement system (PPMS) and a Quantum Design MPMS-SS (SQUID). The susceptibility was measured in a field of 1000 Oe with zero-field cooling in the temperature range of $2\text{--}300 \text{ K}$. Diamagnetic correction was applied for the sample container. Magnetic measurements were performed for 13 samples of $\text{La}_4\text{Cu}_{3-x}\text{Zn}_x\text{MoO}_{12}$ ($x = 0.0, 0.05, 0.10, 0.15, 0.20, 0.30, 0.60, 0.80, 1.00, 1.30, 1.60, 2.00, 2.30$).

Results

$\text{La}_4\text{Cu}_{3-x}\text{Zn}_x\text{MoO}_{12}$ System. Zinc can substitute extensively for copper in the $\text{La}_4\text{Cu}_{3-x}\text{Zn}_x\text{MoO}_{12}$ system up to $x = 2.40$ as shown in Figure 1 (see the Supporting Information for details on lattice parameters of the whole system). However, the substitution is not uniform but consists of two solid solutions with slightly different structural properties. For convenience, we name these solid solutions as SS1 ($0.05 \leq x \leq 0.20$) and SS2 ($0.30 \leq x \leq 2.40$). It can be seen that the unit cell volume varies linearly with the content of Zn substitution within the two solid solutions but has a discontinuous change across the two-phase region.^{21,22} The two-phase region is quite narrow ($0.20 < x < 0.30$), and only two samples ($x = 0.25, 0.28$) are mixtures of SS1 and SS2. The upper limit of Zn substitution in SS2 is about $x = 2.40$, and beyond this limit, another multiphase region was observed, which contains both SS2 and some other unknown phases.

Structure of SS1. Three different polymorphs were known for $\text{La}_4\text{Cu}_3\text{MoO}_{12}$, i.e., hexagonal (h -), orthorhombic (o -), and monoclinic (m -) types.¹⁴ The hexagonal and orthorhombic polymorphs are high-temperature phases and were obtained by quenching, whereas the monoclinic phase is a low-temperature phase which was synthesized by slow cooling. All these polymorphs can be considered as superstructures of the hexagonal YAIO_3 ; thus, their X-ray powder diffraction patterns are rather similar. In Figure 2, we show the SAED patterns for two typical samples, $\text{La}_4\text{Cu}_{2.9}\text{Zn}_{0.1}\text{MoO}_{12}$ (in SS1) and $\text{La}_4\text{Cu}_3\text{MoO}_{12}$. The electron diffraction patterns of $\text{La}_4\text{Cu}_3\text{MoO}_{12}$ can

- (18) Torii, Y.; Matsumoto, H. *Yogyo Kyokaishi* **1975**, *83*, 159–162.
 (19) Larson, A. C.; Von Dreele, R. B. General Structure Analysis System (GSAS), Los Alamos National Laboratory Report LAUR 86-748; Los Alamos, NM, 2004.
 (20) Rietveld, H. M. *J. Appl. Crystallogr.* **1969**, *2*, 65–71.
 (21) Vegard, L. *Z. Phys.* **1921**, *5*, 17.
 (22) Vegard, L. *Kristallogr.* **1928**, *67*, 2399.
 (23) Azuma, M.; Odaka, T.; Takano, M.; Vander Griend, D. A.; Poeppelmeier, K. R.; Narumi, Y.; Kindo, K.; Mizuno, Y.; Maekawa, S. *Phys. Rev. B* **2000**, *62*, R3588–3591.

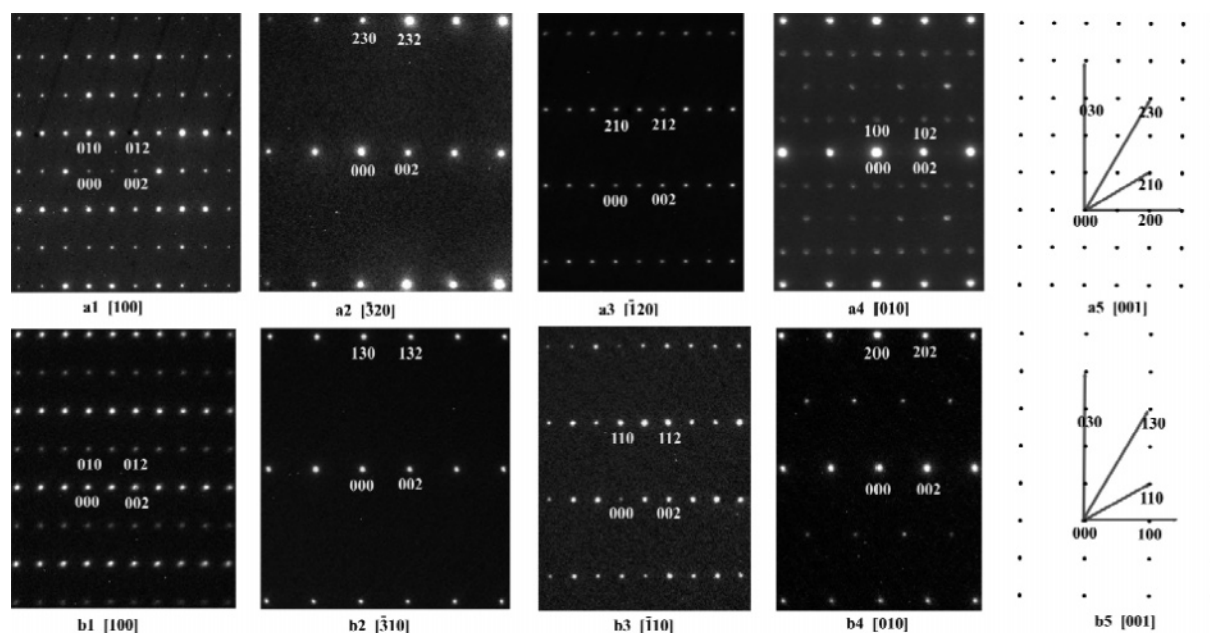


Figure 2. SAED patterns of $\text{La}_4\text{Cu}_3\text{MoO}_{12}$ (a_1, a_2, a_3, a_4, a_5) and $\text{La}_4\text{Cu}_{2.9}\text{Zn}_{0.1}\text{MoO}_{12}$ (b_1, b_2, b_3, b_4, b_5). $a_1, a_2, a_3, a_4; b_1, b_2;$ and b_3, b_4 , are the pair patterns when the samples rotate about the c -axis in 30° steps. a_5 and b_5 are the calculated patterns from a_1, a_2, a_3, a_4 and b_1, b_2, b_3, b_4 , respectively, to show the difference of the two phases.

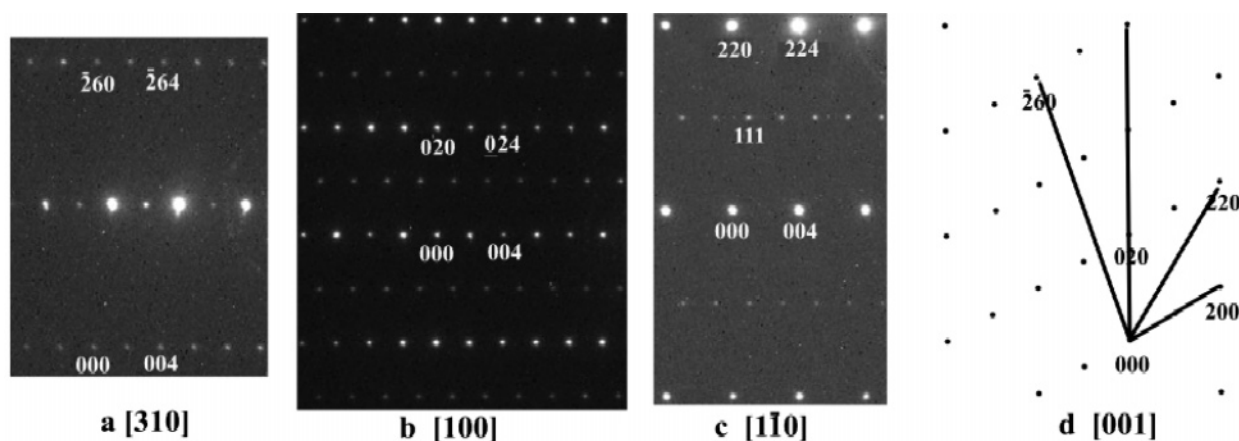


Figure 3. SAED patterns for $\text{La}_4\text{Cu}_2\text{ZnMoO}_{12}$ in the (310) (a), (100) (b), and ($\bar{1}10$) (c) zones; (d) shows the orientation of the diffraction patterns. (The diffraction patterns were indexed using the A-centered pseudo-hexagonal cell, $a = 7.9 \text{ \AA}$ and $c = 22 \text{ \AA}$.)

be indexed with a cell, $a \approx 8.0$, $b \approx 6.9$, $c \approx 11 \text{ \AA}$ and $\gamma \approx 90^\circ$, in the space group $P112_1/m$, indicating that the low-temperature m -polymorph could be formed under the present reaction conditions. The Zn-substituted sample, $\text{La}_4\text{Cu}_{2.9}\text{Zn}_{0.1}\text{MoO}_{12}$, on the other hand, crystallizes in the orthorhombic structure, $a \approx 3.96$, $b \approx 6.86$, $c \approx 11.02 \text{ \AA}$, in the space group $Pmnm$, which is the high-temperature o -polymorph.¹⁴ This means that substitution of Zn to Cu in the system may stabilize the high-temperature modification of the structure. The Rietveld refinement indicates the structure of SS1 fits to the orthorhombic model very well ($R_p \approx 0.07$, $R_{wp} \approx 0.09$ and $\text{GOF} \approx 2.9$, see the details in the Supporting Information). In principle, there should be a boundary between SS1 and m - $\text{La}_4\text{Cu}_3\text{MoO}_{12}$. However, the structures of these two phases are symmetry related, and hence, the boundary of this possible second-order phase transition is difficult to be identified by X-ray diffraction study.

Structure of SS2. The SS2 structures appear for the high Zn content in the $\text{La}_4\text{Cu}_{3-x}\text{Zn}_x\text{MoO}_{12}$ system. Although the X-ray powder diffraction patterns of SS2 are rather similar to

that of the SS1, these two solid solutions are clearly separated by a two-phase region and different slopes of the cell volume as shown in Figure 1. This means that the two solid solutions may have a similar framework but different structures. Figure 3 shows the electron diffraction patterns for $\text{La}_4\text{Cu}_2\text{ZnMoO}_{12}$, and one can clearly see the difference from the o - and m -polymorphs (Figure 2). The diffraction patterns can be indexed with a pseudo-hexagonal cell, $a = 7.94 \text{ \AA}$, $c = 22.04 \text{ \AA}$. The (100) zone reflections follow $k + l = 2n$ indicating a possible A-centered lattice. The diffraction patterns in other zones, (310) and ($\bar{1}10$), confirm the A-centered lattice for $\text{La}_4\text{Cu}_2\text{ZnMoO}_{12}$. The A-centered pseudo-hexagonal cell is not a standard setting and can be expressed with a triclinic cell. The triclinic cell parameters were refined with X-ray diffraction to $a = 11.7114(6) \text{ \AA}$, $b = 11.7098(6) \text{ \AA}$, $c = 7.9329(4) \text{ \AA}$, $\alpha = 80.26(1)^\circ$, $\beta = 99.76(1)^\circ$, $\gamma = 39.60(1)^\circ$.

The triclinic structure model was established by symmetry degradation from the high-temperature hexagonal structure and refined by using both powder X-ray and neutron diffraction data. The structure consists of 6 La, 1 Mo, 3 T (Cu + Zn), and 12 O

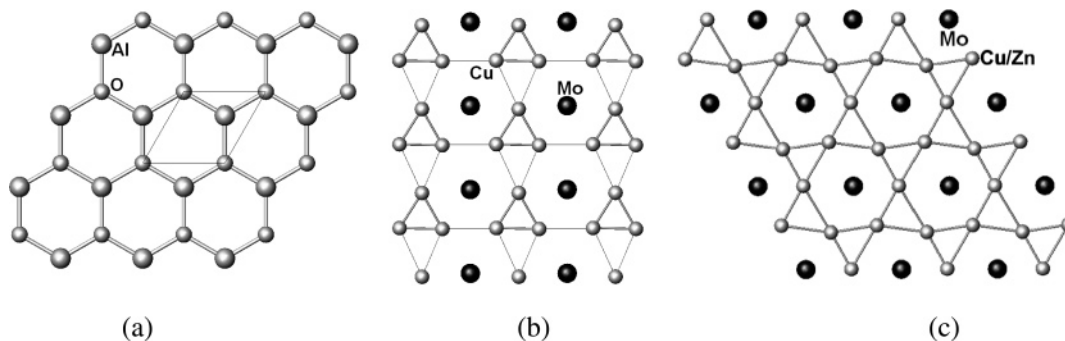


Figure 4. The graphite-like layer in hexagonal the YAIO_3 -type structure (a); the large balls are Al and smaller ones are O. The transition metal atom net in the monoclinic $\text{La}_4\text{Cu}_3\text{MoO}_{12}$ (b) and triclinic $\text{La}_4\text{Cu}_2\text{ZnMoO}_{12}$ (c); the black balls are Mo and lighter ones are Cu (Zn) atoms.

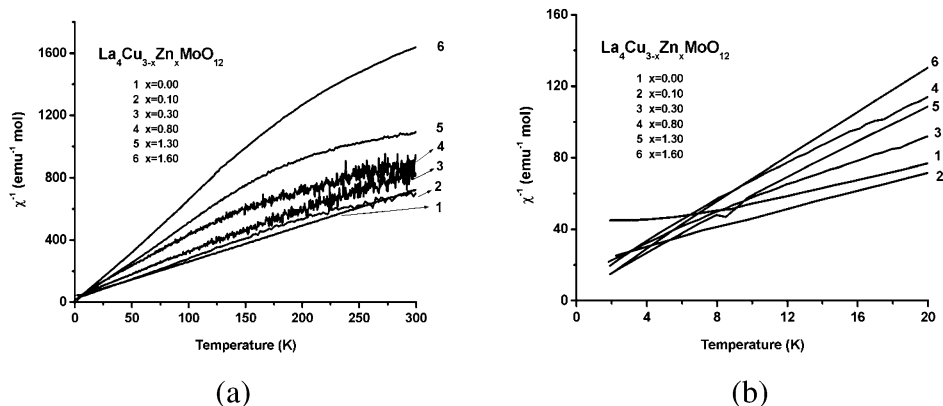


Figure 5. Temperature dependence of the inverse magnetic susceptibility of the $\text{La}_4\text{Cu}_{3-x}\text{Zn}_x\text{MoO}_{12}$ system (a) and the enlarged curves for 0–20 K (b).

Table 1. Effective Magnetic Moments Calculated from $\chi^{-1}(T)$ between 15 and 150 K

x in $\text{La}_4\text{Cu}_{3-x}\text{Zn}_x\text{MoO}_{12}$	0	0.15	0.3	0.6	0.8	1.0	1.3	2.0	2.3
free electrons per formula	1.04	0.96	0.94	0.75	0.76	0.67	0.61	0.36	0.24
free electrons per 3 Cu	1.04	1.02	1.04	0.94	1.03	1.01	1.08	1.08	1.04

positions. The substituted Zn atoms are randomly distributed in the three T positions. One should keep in mind that the diffraction technique provides only the long-range information; thus, we cannot exclude the short-range order of the cations in the structure, and as we will show below, the short-range ordering is very important to understand the magnetic properties of these materials. Crystallographic data, refined atomic parameters, and Rietveld plots are listed in the Supporting Information.

The structures in the $\text{La}_4\text{Cu}_{3-x}\text{Zn}_x\text{MoO}_{12}$ system are all related to the hexagonal YAIO_3 -type, in which the transition metal ions occupy trigonal bipyramid sites forming a transition metal and oxygen sheet (TO_3 sheet) with the lanthanum ions located in between. In the hexagonal YAIO_3 structure, the aluminum and an oxygen atom form a graphite-like layer (AlO), in which the Al and O alternate (Figure 4a). For $\text{La}_4\text{Cu}_3\text{MoO}_{12}$, since the charges of Mo^{VI} and Cu^{II} are significantly different, they may occupy independent sites in the structure. It was known that the Mo^{VI} and Cu^{II} ions are randomly distributed in the h - $\text{La}_4\text{Cu}_3\text{MoO}_{12}$, partially ordered in the o -polymorph, and completely ordered in the low-temperature m -polymorph.¹⁴ In the triclinic structure of $\text{La}_4\text{Cu}_2\text{ZnMoO}_{12}$ (t -polymorph), the Mo^{VI} and $\text{Cu}^{\text{II}}/\text{Zn}^{\text{II}}$ ions are also ordered but in a different fashion from the m -polymorph. In Figure 4, parts b and c, we show the arrangements of the transition metal ions in the $[\text{TO}_3]$ layers in the m - and t -polymorphs. The oxygen ions are omitted for clarity. However, one should keep in mind that all of these

transition metal ions are coordinated by oxygen ions with a distorted trigonal bipyramid. It can be seen that the transition metal ions in $[\text{TO}_3]$ form a close-packed layer in both m - and t -polymorphs, in which the Mo and Cu/Zn ions are ordered. The Cu^{II} ($\text{Cu}^{\text{II}}/\text{Zn}^{\text{II}}$) ions form trigonal units, which link to chains by sharing edges and corners in m - $\text{La}_4\text{Cu}_3\text{MoO}_{12}$ and a (6, 3) net by sharing corners in t - $\text{La}_4\text{Cu}_2\text{ZnMoO}_{12}$, while the Mo^{VI} ions are located at the center of hexagon in both structures. The $[\text{TO}_3]$ layers are stacked one after another, and between them the lanthanides are located forming 3-dimensional structures.

Magnetism of SS1 and SS2. As indicated above, all structures in the $\text{La}_4\text{Cu}_{3-x}\text{Zn}_x\text{MoO}_{12}$ system contain a Kagomé-like lattice consisting of corner-sharing triangular clusters of Cu^{II} and Zn^{II} ions. Zn^{II} is a nonmagnetic ion; therefore, the Zn substitution may influence the magnetic interaction of the Kagomé lattice in the systems. Figure 5 shows the inverse magnetic susceptibilities ($1/\chi_{\text{mol}}$) with temperature of the $\text{La}_4\text{Cu}_{3-x}\text{Zn}_x\text{MoO}_{12}$ system. The magnetic susceptibility follows the Curie–Weiss law between 15 and 150 K for all samples but deviates beyond this temperature range. The effective magnetic moments calculated from the slope of $1/\chi_{\text{mol}}$ with temperature are listed in Table 1. The number of free electrons per 3 Cu is close to one for all samples indicating that the system can be well expressed by independent $[\text{Cu}^{\text{II}}_3]$ clusters. The linear correlation of $1/\chi_{\text{mol}}$ with temperature means that the magnetic interaction is strong within the $[\text{Cu}^{\text{II}}_3]$ cluster but very weak between the clusters in this temperature region. Above 150 K,

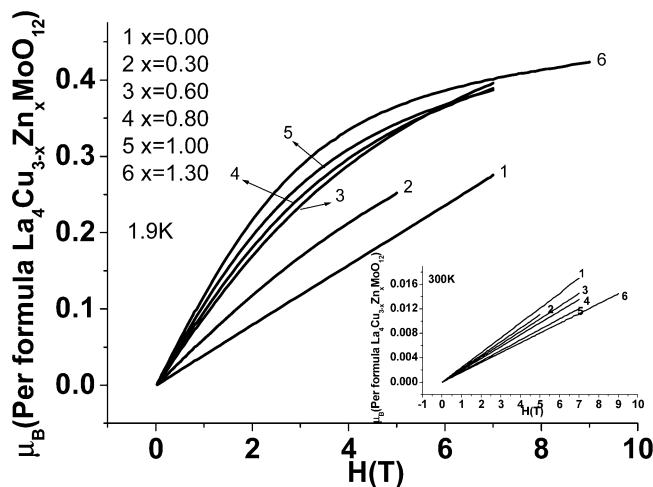


Figure 6. Magnetization (per formula unit) as a function of applied field for SS2.

the inverse magnetic susceptibility $1/\chi_{\text{mol}}$ shows a downward deviation from linear, and furthermore, as the Zn content increases the deviation temperature decreases. The $1/\chi_{\text{mol}}$ curve is almost linear for $\text{La}_4\text{Cu}_3\text{MoO}_{12}$, but as indicated by Vander Griend et al., $\text{La}_4\text{Cu}_3\text{MoO}_{12}$ also exhibits similar behavior above 300 K.¹⁴ This downward variation represents the crossover from triangular Cu^{II} clusters to the paramagnetic state of the isolated Cu^{II} .

Below 15 K, the inverse magnetic susceptibility also deviates from the Curie–Weiss law. As shown in Figure 5b, $1/\chi_{\text{mol}}$ goes upward at low temperature for $\text{La}_4\text{Cu}_3\text{MoO}_{12}$, almost linear for the low Zn content sample ($x = 0.10$), and downward for the high Zn content samples in the $\text{La}_4\text{Cu}_{3-x}\text{Zn}_x\text{MoO}_{12}$ system. The $\text{La}_4\text{Cu}_3\text{MoO}_{12}$ was known to exhibit nonhysteretic antiferromagnetic behavior at low temperature ($T_N = 5$ K).²³ The downward deviation of the $1/\chi_{\text{mol}}$ curves for the high Zn content samples indicates that the substitution of Zn^{II} in this system induces ferromagnetic interaction between the $[\text{Cu}^{\text{II}}_3]$ clusters. The presence of long-range magnetic interaction in the $\text{La}_4\text{Cu}_{3-x}\text{Zn}_x\text{MoO}_{12}$ system is further evidenced by magnetization measurements (Figure 6). The magnetization of $\text{La}_4\text{Cu}_3\text{MoO}_{12}$ is almost linearly proportional to the magnetic field at 1.9 K and room temperature. For the Zn-substituted $\text{La}_4\text{Cu}_{3-x}\text{Zn}_x\text{MoO}_{12}$ samples, on the other hand, the magnetization curves show linear dependence on the magnetic field at room temperature but exhibit saturation behavior at 1.9 K. Furthermore, the Zn-substituted samples ($\text{La}_4\text{Cu}_2\text{ZnMoO}_{12}$) also show small hysteresis, as shown in Figure 7, implying the presence of spontaneous magnetization in the material. The neutron diffraction data collected at 10 K shows that magnetic diffraction peaks are overlapped with the nuclear peaks, which agrees well with such spontaneous magnetization (see the Supporting Information for details).

Discussion

It was known that three different structures were found for $\text{La}_4\text{Cu}_3\text{MoO}_{12}$, i.e., the *h*-, *o*-, and *m*-polymorphs.¹⁴ The *h*-polymorph is a high-temperature form, in which the Mo and Cu ions are randomly distributed in a single site. The symmetry degradation of the low-temperature polymorphs originates from the ordering of the Mo and Cu ions. The transition metal ions are partially ordered in the orthorhombic form (*o*-polymorph)

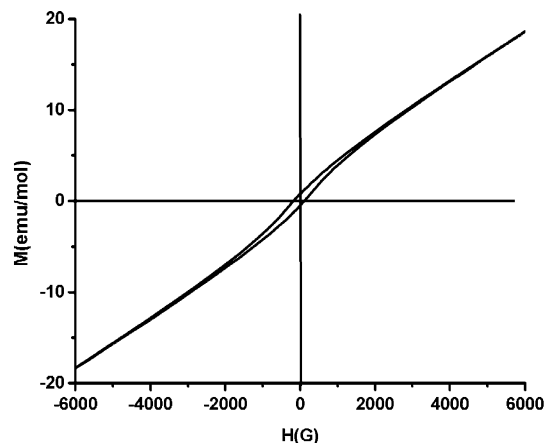
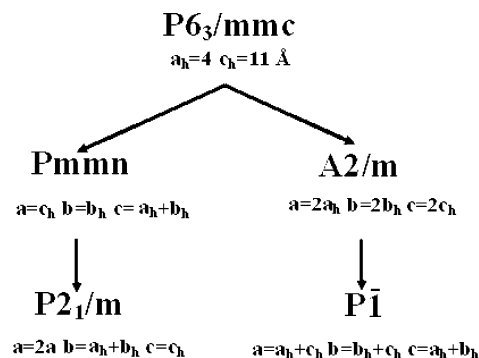


Figure 7. The M – H loop for $\text{La}_4\text{Cu}_2\text{ZnMoO}_{12}$ at 10 K.

Scheme 1



and completely ordered in the *m*-polymorph. Although the long-range order (LRO) is different for these phases, they follow the symmetry tree, $P6_3/mmc \rightarrow Pmmm \rightarrow P2_1/m$. Therefore, the transformation between these structures might be a second-order phase transition, and this is the reason that one cannot identify the phase boundary between $\text{La}_4\text{Cu}_3\text{MoO}_{12}$ and SS1. As far as the symmetry is concerned, the triclinic (*A*-centered pseudohexagonal) structure found for the Zn-substituted samples (SS2) could also be regarded as a low-temperature polymorph of this system. The triclinic structure can also be derived from the high-temperature hexagonal structure but through another pathway. In Scheme 1, we show their symmetry relationship. From the crystal structure of the *t*-polymorph, we knew that the ordering of Mo and Cu/Zn ions is different from that of the *m*-polymorph; therefore, the structure of SS2 is an independent symmetry-related derivative of the *h*-polymorph and is well separated from *m*-polymorph in the phase diagram. As indicated, all the structures in this system have the same framework (topologically); the only difference is the ordering arrangement.

The symmetry relationship between the *t*- and *h*-polymorphs is also evidenced by the presence of twins in the samples. In Figure 8 we show the SAED patterns and the high-resolution TEM (HRTEM) image of $\text{La}_4\text{Cu}_2\text{ZnMoO}_{12}$. The particle selected is a twin crystal, in which the twin components are stacked along the *c*-axis of the pseudohexagonal cell. The diffraction patterns shown in Figure 8, parts a and b, were obtained by Fourier transformation from selected areas of the HRTEM, which correspond to different components of the twin crystal. On the basis of the pseudohexagonal cell, the twin operation can be expressed as the following:

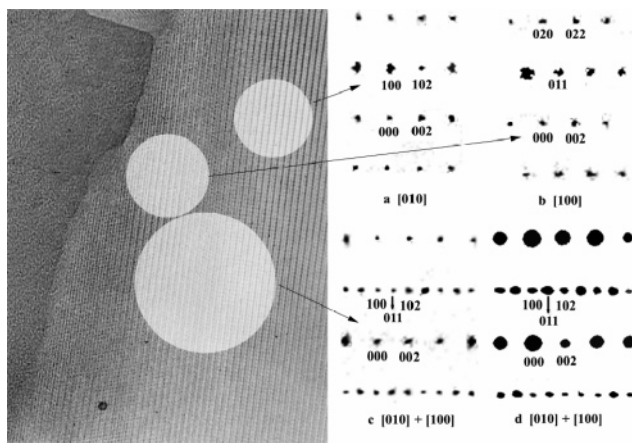


Figure 8. High-resolution TEM image for $\text{La}_4\text{Cu}_2\text{ZnMoO}_{12}$; (a–c) are the selected area Fourier transforms and (d) is an observed electron diffraction (SAED) pattern. (The diffraction patterns were indexed using the A-centered pseudo-hexagonal cell, $a = 7.9 \text{ \AA}$ and $c = 22 \text{ \AA}$.)

$$(a', b', c') = \begin{pmatrix} 0 & 1 & 0 \\ 1 & 0 & 0 \\ 0 & 0 & 1 \end{pmatrix} (a, b, c) \quad (1)$$

With the use of the large area image, the Fourier transformation leads to a diffraction pattern (Figure 8c), which is the superposition of the two components of the twin crystal as often observed in the experiments (Figure 8d). The formation of the twins in the t -polymorph can be understood by symmetry degradation from the h -polymorph. In the h -polymorph, the Mo and Cu/Zn ions are randomly distributed. During the cooling, the Mo and Cu/Zn ions become ordered. Since the a and b axes are equivalent in the hexagonal structure, the cation ordering can go in either the a - or b -directions, which leads to formation of the twins.

In the structure refinement, we assumed that the Cu and Zn ions are disordered. This is valid only in the scale of the coherence length of the incident radiation (X-ray or neutron). One could not, however, exclude the short-range ordering of Cu and Zn ions in the structure. An interesting finding is that the effective magnetic moment is about one electron per 3 Cu in the whole solid solution (Table 1). Assuming that Cu and Zn ions are randomly distributed (referred as the “random model”), part of the copper atoms in the Cu^{II}_3 should be replaced by zinc; in such a case, there should be $(1 - y)^3 [\text{Cu}^{\text{II}}_3]$, $3(1 - y)^2y [\text{Zn}^{\text{II}}\text{Cu}^{\text{II}}_2]$, $3(1 - y)y^2 [\text{Zn}_2^{\text{II}}\text{Cu}^{\text{II}}]$, and $y^3 [\text{Zn}^{\text{II}}_3]$ per $\text{La}_4\text{Cu}_{3-x}\text{Zn}_x\text{MoO}_{12}$ with $y = \text{Zn}/(\text{Zn} + \text{Cu})$. Since only Cu^{II} has substantial contribution to the magnetic interaction, one would expect that $[\text{Zn}^{\text{II}}\text{Cu}^{\text{II}}_2]$ and $[\text{Zn}^{\text{II}}_3]$ clusters have no contribution to the magnetism. Therefore, the system should not follow the rule of “one electron per 3 Cu”. It seems that the Cu^{II} and Zn^{II} ions tend to form clusters separately, i.e., $[\text{Cu}^{\text{II}}_3]$ and $[\text{Zn}^{\text{II}}_3]$, in this system (referred as the “separate cluster model”). Figure 9 shows the effective moments of the $\text{La}_4\text{Cu}_{3-x}\text{Zn}_x\text{MoO}_{12}$ system. The solid line is the calculated value from separate cluster model. The dashed line in the figure is the calculated value from random model. Obviously, the separate cluster model shows a better fit to the magnetic moment data (see the Supporting Information for details).

The $\text{La}_4\text{Cu}_{3-x}\text{Zn}_x\text{MoO}_{12}$ is a unique system in which the copper ions tend to form homoatomic clusters. In the Zn-substituted systems, Cu^{II} and Zn^{II} form Cu^{II}_3 and Zn^{II}_3 clusters

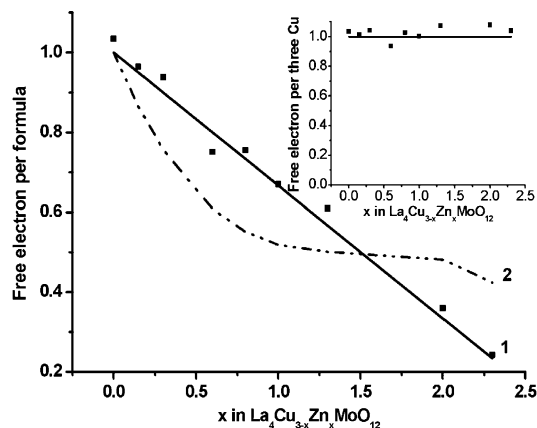


Figure 9. Free electrons (per formula) for SS1 and SS2 at low temperature (about 20–150 K). Curve 1 is for the separate cluster model, and curve 2 is for the random model. Inset shows free electrons per three Cu atoms.

separately. In the temperature range of 15–150 K, the magnetic interaction within the Cu^{II}_3 cluster is sufficient to behave as an $S = 1/2$ species. Such a system is more or less similar to the spin glass, in which the magnetic species are separated by a nonmagnetic matrix. It is well established that the magnetic interactions in spin glass depend crucially on the average distance between the magnetic species, which may oscillate in being either antiferro- or ferromagnetic. The $\text{La}_4\text{Cu}_{3-x}\text{Zn}_x\text{MoO}_{12}$ system represents nicely the spin glass behavior. The Zn substitution dilutes the magnetic Cu^{II}_3 clusters, and as the Zn content increases, the magnetic interaction between the Cu^{II}_3 clusters changes from antiferromagnetic for $\text{La}_4\text{Cu}_3\text{MoO}_{12}$ to paramagnetic for the low Zn content samples and then to weak ferromagnetic for the high Zn content samples.

Conclusions

By standard solid-state reactions Zn can be substituted for Cu in $\text{La}_4\text{Cu}_3\text{MoO}_{12}$ to form two solid solutions SS1 with $0.05 \leq x \leq 0.20$ and SS2 with $0.30 \leq x \leq 2.40$ in the series $\text{La}_4\text{Cu}_{3-x}\text{Zn}_x\text{MoO}_{12}$ ($0 \leq x \leq 2.6$). They all belong to the “ YAlO_3 ” type compound where copper, zinc, and molybdenum are five-coordinate, crystallized in the space group $Pmnm$ and $P-1$, respectively. In the transition metal cations layer, the copper and zinc cations order into a Kagomé-like lattice of triangular clusters that tend to consist of pure Cu^{II}_3 clusters and Zn^{II}_3 clusters, confirmed by the result that the number of free electrons per 3 Cu is close to one for all samples in SS1 and SS2. This is the main cause of the spontaneous magnetization observed in the system.

Acknowledgment. This work is supported by the National Natural Science Foundation of China (Grant 20471003).

Supporting Information Available: Conductivity data, synthesis temperatures, lattice parameters, and Rietveld refinement details of the $\text{La}_4\text{Cu}_{3-x}\text{Zn}_x\text{MoO}_{12}$ system and some discussions on the ferromagnetic moment and the random and separate cluster model of Cu and Zn in the Kagomé lattice. This material is available free of charge via the Internet at <http://pubs.acs.org>.

JA053489A